FUNDAMENTALS & APPLICATIONS

CHEMELECTROCHEM

ANALYSIS & CATALYSIS, BIO & NANO, ENERGY & MORE

Accepted Article

Title: Manganese (II,III) oxide-activated carbon black supported PtRu nanoparticles for methanol electrooxidation in acid medium

Authors: Juan Manuel Sieben, Vanina Comignani, Maximiliano Brigante, and Marta M.E. Duarte

This manuscript has been accepted after peer review and appears as an Accepted Article online prior to editing, proofing, and formal publication of the final Version of Record (VoR). This work is currently citable by using the Digital Object Identifier (DOI) given below. The VoR will be published online in Early View as soon as possible and may be different to this Accepted Article as a result of editing. Readers should obtain the VoR from the journal website shown below when it is published to ensure accuracy of information. The authors are responsible for the content of this Accepted Article.

To be cited as: *ChemElectroChem* 10.1002/celc.201800413

Link to VoR: http://dx.doi.org/10.1002/celc.201800413

A Journal of

ChemPubSoc Europe

WILEY-VCH

www.chemelectrochem.org

WILEY-VCH

ARTICLE

Manganese (II,III) oxide-activated carbon black supported PtRu nanoparticles for methanol electrooxidation in acid medium

Vanina Comignani[a], Juan Manuel Sieben*[a], Maximiliano E. Brigante[b], Marta M.E. Duarte[c]

Abstract: In this work, PtRu nanoparticles supported on hybrid manganese(II,III)-carbon composites were prepared by microwave-assisted polyol process with ethylene glycol. The obtained PtRu/(100-x)C.xMn_3O_4 catalysts were characterized by XRD diffraction, TEM, SEM-EDX analysis, ICP-AES and electrochemical techniques. Small and well-distributed nanoparticles of about 2.6 nm were obtained over the hybrid support. The as-prepared catalysts presented similar Pt:Ru atomic ratio (ca. 3.4:1), indicating that the composition of the bimetallic system is unaffected by the oxide content in the hybrid support. However, the noble metal loading increased with the increase in the oxide content due to the formation of more nucleation sites during microwave heating. The electrochemical experiments showed that the best performance and the lowest poisoning rate are obtained with PtRu/90C.10Mn_3O_4 followed by PtRu/70C.30Mn_3O_4. The bimetallic catalyst supported over 90C.10Mn_3O_4 exhibited a steady current density of 215 mA mg_{PtRu}^{-1} at 0.5 V, which is 40 % higher than that of PtRu/C. This behavior is mainly associated with the ability of Mn_3O_4 to provide a large extra amount of hydroxyl groups and promote the dehydrogenation of methanol.

Introduction

Increasing awareness of energy consumption, particularly from fossil fuels, and global warming has prompted researchers to investigate alternative power sources to generate electricity in a much more efficient, cost-effective and environmentally friendly way. Over the last years, focus has been placed on the development of direct methanol (DMFCs) and ethanol fuel cells (DEFCs) technology due to their high energy density. Also these fuels can be obtained from renewable sources. Moreover, they can be easily stored and distributed through the existing fossil fuel infrastructure.[1]

[a] Ing. V. Comignani and Dr. J.M. Sieben
Intituto de Ingeniería Electroquímica y Corrosión and CONICET
Universidad Nacional del Sur
Av. Alem 1253, B8000CPB Bahía Blanca, Argentina
E-mail: jmsieben@uns.edu.ar
[b] Dr. M. Brigante
INQUISUR and Departamento de Química
Universidad Nacional del Sur
Av. Alem 1253, B8000CPB Bahía Blanca, Argentina
[c] Prof. M.M.E. Duarte
Intituto de Ingeniería Electroquímica y Corrosión
Universidad Nacional del Sur
Av. Alem 1253, B8000CPB Bahía Blanca, Argentina

To obtain the maximum benefit from alcohol fuels many options have been explored, such as different catalytic structures, combination of metals, substrates and modifications of the fuel cell stack hardware. In general, the different proposals aim to improve the reaction kinetics and achieve a greater electrochemical area to carry out the oxidation of the alcohols at a lower cost.

Among the pure metals, platinum is the best electrocatalyst for the oxidation of many alcohols in low-temperature fuel cells. However, Pt is very expensive, scarce in nature and easily poisoned due to the presence of CO and other intermediate species strongly adsorbed on its surface. Specifically, in methanol electrooxidation, active sites are occupied with intermediate species, such as CO, and stop the long-term activity of the catalyst.[2] Besides, when CO molecules are strongly adsorbed on the platinum surface, the anodic potential rises more than the thermodynamic value needed to obtain reasonable reaction rate.[3,4] Several investigation groups have explored different ways to combine Pt with other metals in order to facilitate the energy generation. A good choice is to alloy Pt with more oxophilic elements such as Ru, Sn, Mo, Co, Ni, etc. [5,6] A facile and rapid method to synthetize Pt-based nanoparticles is the microwave-assisted technique. This technique is an effective way to obtain nanosized catalysts.[7,8] The radiation provides a faster and homogenous heating of the reaction medium than other synthesis methods.[9] Moreover, it is known that the active nucleation sites are generated when some substrates are irradiated by microwaves because of the temperature difference between medium and substrate surface. [10]

Another approach to enhance the electrocatalytic activity of Pt-based catalysts towards methanol oxidation consists in adding metal oxides, nitrides and carbides to the carbonaceous material (i.e., to form a hybrid support).[11,12] The incorporation of another oxophilic compound in the substrate cannot only maximize the performance of the electrode but also improves the economic efficiency of DMFCs. Furthermore, the hybrid support can help to reduce considerably the noble metal loading and promote the oxidation of the poisoning intermediates at the platinum sites. Specifically, metal oxides are capable of improving the Pt particle dispersion, as well as modifying their electronic structure.[13,14] In addition, the metal oxides can enhance the dissociative adsorption of water at lower potentials than Pt surface alone. That is, the OH species generated onto them are capable of facilitating the oxidation of adsorbed CO to CO_2.[15] In this regard, recent investigations have shown that mixed oxides of manganese are promising candidates for use in hybrid catalyst supports because they have enough electrochemical surface reactivity to increase the population of surface species such as H_{ad} atoms and OH_{ad} groups.[16-18]

Accepted Manuscript

This article is protected by copyright. All rights reserved.

The aim of this work is to synthetize PtRu nanoparticles on hybrid supports conformed by manganese(II,III) oxide and carbon black with different compositions. The bimetallic PtRu nanoparticles were synthesized by the microwave-assisted polyol process and the as-prepared PtRu/(100-x)C.xMn_3O_4 catalysts were characterized by X-ray diffraction, energy dispersive X-ray spectroscopy, transmission electron microscopy and inductively coupled plasma atomic emission spectroscopy. The electrocatalytic performance of the as-prepared samples for methanol oxidation in acid medium was investigated by conventional electrochemical techniques. The influence of Mn_3O_4 nanoparticles on the electrocatalytic activity of the bimetallic system is discussed in detail.

Results and Discussion

The XRD patterns of the different catalysts are displayed in Fig. 1. All samples show major diffraction peaks at *2θ* values of about 40 and 47 ° associated with the (111) and (200) planes, which belong to the family of crystal planes of the platinum face centered cubic structure (*fcc*). In addition, M10, M30 and M50 catalysts also present peaks corresponding to the tetragonal structure of manganese (II,III) oxide located at Bragg angles of 32.3, 36.1 and 59.9 ° which correspond to the (103), (211) and (224) planes, respectively. Regarding the diffraction peaks associated with Pt (Table 1), a slight shift to higher *2θ* values was observed indicating that the particles are composed of a PtRu alloy. The latter can justify the absence of Ru diffraction peaks. Moreover, no appreciable changes were observed in the diffraction peaks of Mn(II,III) oxide after synthesis process.

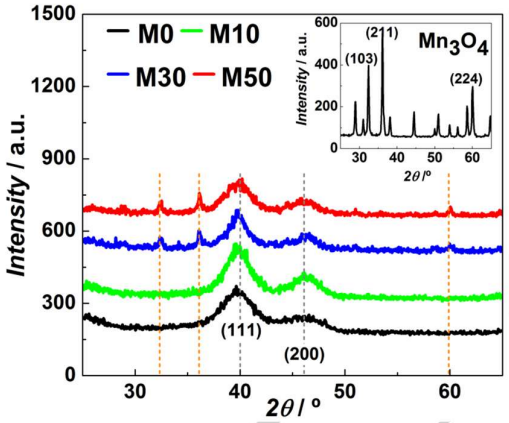

Figure 1. XRD patterns of the as-prepared catalysts.

TEM image of manganese oxide is shown in Fig. 2 revealing predominant octahedral morphology. The particle size of the composite ranged between 20 and 40 nm, which was very similar to the carbon support. Fig. 3 shows the TEM micrographs of the bimetallic nanoparticles supported on the hybrid materials and their respective histograms of particle size distribution. The PtRu nanoparticles presented spherical morphology with diameters of less than 3 nm. It was found that the particle distribution depends on the oxide content in the support, although no clear dependence was seen between the particle size and the oxide content. The biggest mean particle size was obtained on the carbon support (2.94 nm for M0), while the smallest mean size was achieved on the 50C.50Mn_3O_4 (2.55 nm for M50) (Table 1). Regarding particle distribution, agglomerates were observed in M0 sample. As shown by TEM images and the corresponding size distributions, the particle distribution becomes more uniform with the addition of Mn_3O_4. Thus uniformly distributed PtRu nanoparticles were obtained over the entire surface when a hybrid support was used, possibly due to the oxophilic nature of Mn_3O_4 and the increment in the number of nucleation centers for formation of nanoparticles, as has been proposed by Nouralishahi et al. for Pt/MWCNT electrocatalysts.[10] However, the presence of the metal oxide is not the only cause for improving particle dispersion. The synthesis method also plays an important role to achieve those characteristics, since microwave radiation allows a fast and uniform heating of the reaction medium. According to Anumol et al. complementary studies demonstrated that microwave radiation results in enhanced reaction kinetics and leads to the formation of products with uniform size and shape.[9]

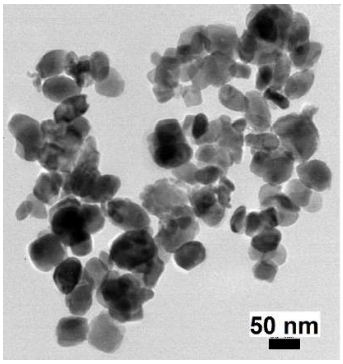

Figure 2. TEM image of Mn_3O_4 oxide nanoparticles.

Accepted Manuscript

This article is protected by copyright. All rights reserved.

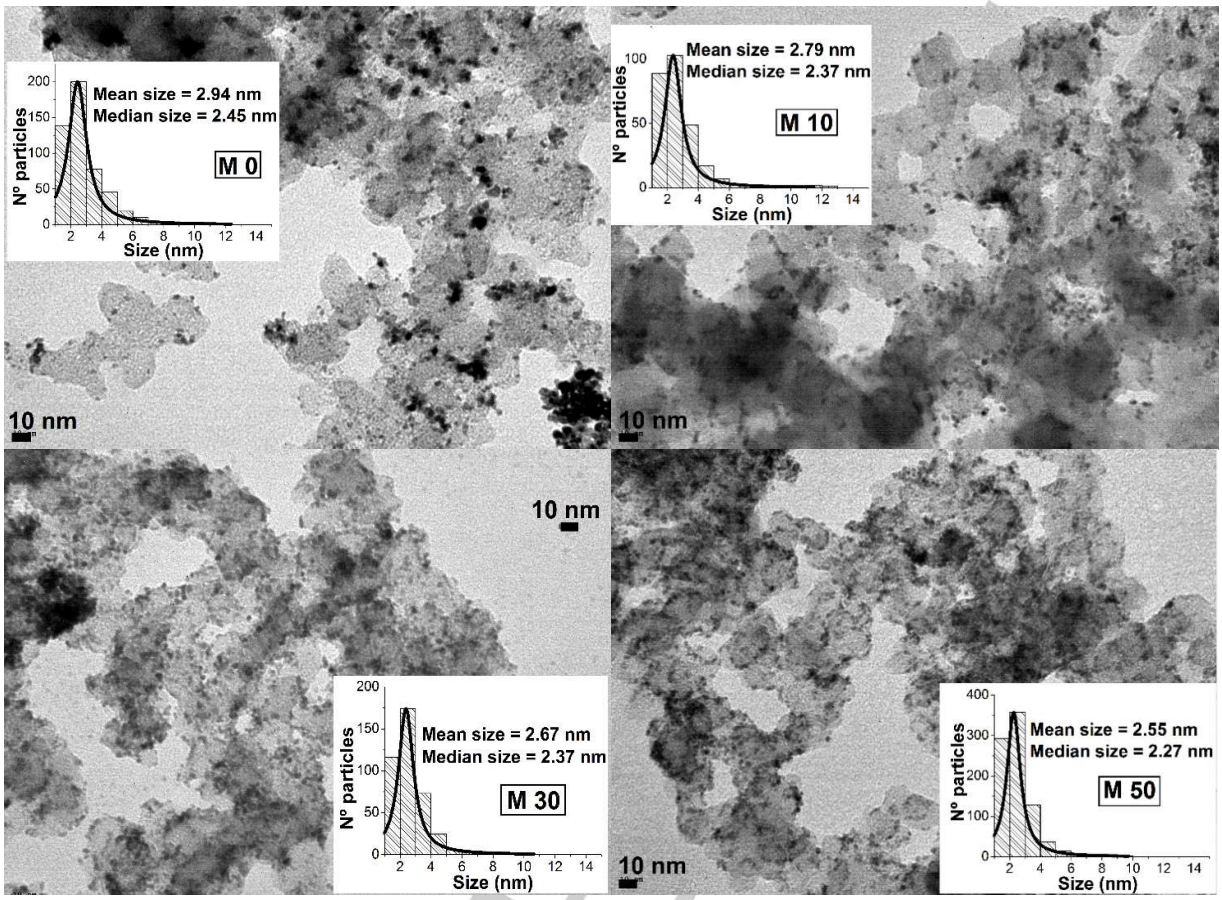

Figure 3. TEM images and histograms of particle size distributions of M0, M10, M30 and M50 catalysts.

Catalysts compositions were determined by EDX and ICP-AES analysis and the results are summarized in Table 2. The different catalysts have similar Pt:Ru atomic ratio, around 3.4:1. This indicates that the composition of the bimetallic system is unaffected by the oxide content in the hybrid support. Moreover, the ICP-AES studies revealed that the increase in Mn_3O_4 content leads to a higher loading of the noble metals nanoparticles. This increment in catalyst loading can be attributed to the formation of more nucleation sites where Pt and Ru ions can be reduced during the microwave heating. The latter results are in agreement with those obtained by Anumol et. Al [9], who also examined the relationship between the nature of support and the number of nucleation sites.

Table 1. Characteristic parameters of the as-prepared PtRu/(100-x)C.xMn_3O_4 catalysts.

Catalyst	(111) peak 2θ	a_{fcc} Å	d_p (TEM) nm	*FWHM*
M0	39.91	3.897	2.9 ± 0.3	3.363 ± 0.128
2.5M10	39.74	3.915	2.8 ± 0.2	2.981 ± 0.047
M30	39.80	3.910	2.7 ± 0.5	1.947 ± 0.085
M50	39.79	3.934	2.6 ± 0.6	2.909 ± 0.077

The catalysts were cycled in 0.5 M H_2SO_4 solution from -0.25 to 1.2 V at a scan rate of 50 mV s^{-1} to examine their electrochemical surface properties. Fig. 4a displays the cyclic voltammetry response of the as-prepared catalysts. The CV curves show the characteristic polycrystalline Pt features: H proton adsorption/desorption pattern (-0.25 to 0.1 V), double layer charge (0.1 to 0.25 V) and formation/reduction of surface platinum

Accepted Manuscript

This article is protected by copyright. All rights reserved.

oxide or Pt-OH_{ad} (0.25 to 1.2 V). The magnitude of the double layer is the main difference between the different systems. The background currents of M10, M30 and M50 are larger than that of M0, probably due to the presence of a higher amount of oxygenated species or a larger surface area related to better particles dispersion and smaller particle size.[19,20] Table 2 confirms that the Pt loading increases as Mn_3O_4 content increases. Furthermore, it must be noted that the incorporation of manganese oxide affects the electrochemical performance of the M10, M30 and M50 catalysts. The oxophilic nature of Mn(II,III) oxide facilitates the formation of -OH_{ad},[10] i.e. behaves like ruthenium,[21] via the following reactions:

$$Mn_xO_{x+1} + H_2O \rightarrow Mn_xO_{x+1}\text{-}OH_{ad} + H^+ + e^- \quad (1)$$

$$Ru + H_2O \rightarrow Ru\text{-}OH_{ad} + H^+ + e^- \quad (2)$$

Thus, the increase of the double layer charge can be attributed essentially to the formation of hydroxylated species generated from water discharge that contribute to the pseudocapacitance of the system.

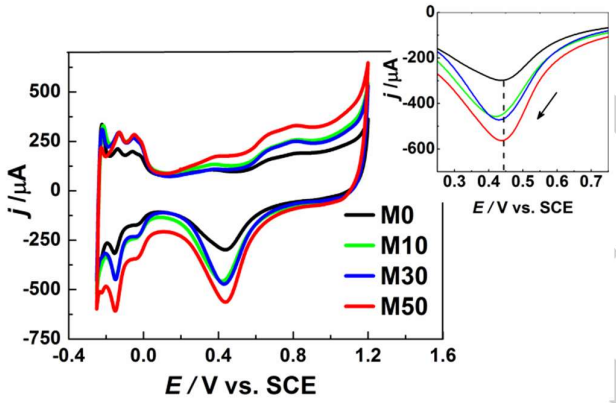

Figure 4. Stabilized cyclic voltammograms of the different electrodes in 0.5 M H_2SO_4 at a sweep rate of 50 mV s^{-1}. The inset shows the magnification of the peak related to the oxides reduction.

Analogously, the participation of Mn_3O_4 not only results in increased background currents but also in significantly increased oxophilicity. During the cathodic sweep, the surface oxides formed during anodic polarization are reduced, restoring the clean metal surface (M). When the interaction M-OH_{ad} is stronger, the applied potential must be lower to restore the metal surface. In the cathodic sweep (Fig. 4b) the peak related to oxide reduction (ca. 0.45 V) shifts towards more negative potentials as the content of Mn_3O_4 increases. This shift can be associated with an increase in the surface oxophilicity and in the population of M-OH_{ad} sites.[22]

On the other hand, a rise in oxophilicity may be also explained by the use of Pt nanoparticles. According to Mayrhofer et al. and Arenz et al. the oxophilicity of platinum particles increases by decreasing the particle size.[23,24] However, in this case, it is more probable that the variation in Mn(II,III) oxide loading rather than the particle size effect is responsible for the change in oxophilicity.[25]

Table 2. Composition of the as-synthesized electrocatalysts.

Catalyst	Composition[a] Pt	Ru	Ratio[a] Pt:Ru	Mn_3O_4 on carbon [b]	Pt loading on GC[c]	ECSA[d]
	at. %			wt. %	μg cm^{-2}	m^2 g^{-1}
M0	82.1	17.9	4.6	0	87.7	54.8
M10	77.1	22.9	3.4	15.1	118.6	69.5
M30	77.1	22.9	3.4	31.7	181.0	70.1
M50	75.8	24.2	3.2	53.8	189.9	73.0

[a] Atomic composition determined by EDX. [b] Mass composition determined by ICP-AES. [c] Platinum loading per unit of GC geometric area. Data from ICP-AES analysis. [d] Electrochemical active surface area per unit mass of Pt and Ru.

Finally, a small anodic peak in the anodic sweep appears at a potential of ca. 0.4 V. It can be seen that the peak intensity increases with the increase in the oxide content. This anodic peak can be ascribed to a faradaic process that involves the intercalation/de-intercalation of H atoms into Mn_3O_4 lattice. The redox reaction that takes place in the oxide can be represented as follows:

$$Mn_xO_{x+1} + H^+ + e^- \rightleftarrows Mn_xO_{x+1}H \quad (3)$$

Similar behavior was observed in other platinum based catalysts supported over different metal oxides, such as WO_3, V_2O_5, Nb_2O_5 and MoO_3.[12,26,27]

The electrochemical active surface area per unit mass of PtRu (*ECSA*) of the as-prepared electrocatalysts can help us to find the key relationship between the structure/composition of the catalyst and their electroactivity in order to develop highly efficient anode materials for direct methanol fuel cells (DMFCs). In general, the *ECSA* values calculated by hydrogen adsorption works well for some metal electrodes. However, there are undefined pseudofaradic contributions in the hydrogen adsorption/desorption region of the as-synthetized catalysts that cannot be eliminated during the cyclic voltammetry experiments. For that reason, the H adsorption region can be distorted and the calculation of the electroactive surface area by this method turns out to be inaccurate. Thus, CO stripping was the method chosen to determinate the active surface area following the steps described in the Experimental Section. The CO stripping voltammograms recorded at a scan rate of 10 mV s^{-1} and room temperature are shown in Fig. 5. The *ECSA* values were calculated according to Equation (4) and compiled in Table 2.

$$ECSA = Q_{CO} / (420 \times w_{PtRu}) \quad (4)$$

Accepted Manuscript

This article is protected by copyright. All rights reserved.

Where Q_{CO} (μC) represents the integrated area under the oxidation peak of the monolayer of adsorbed CO, w_{PtRu} is the Pt and Ru loading (g) of the electrode and 420 μC cm^{-2} represents the charge required to desorb a monolayer of carbon monoxide adsorbed on Pt and Ru.

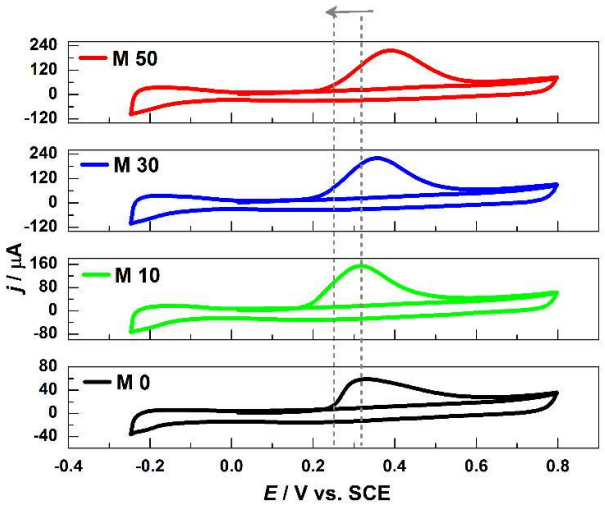

Figure 5. Comparative CO stripping current response of M0, M10, M30 and M50 electrodes.

The *ECSA* value of the Mn_3O_4-free sample is 54.8 m^2 g_{PtRu}^{-1}. Although the (100-x)C.xMn_3O_4 supported catalysts have larger *ECSA* values than M0 sample, not significant differences were observed between them. The *ECSA* values for M10, M30 and M50 samples were calculated to be 69.5, 70.1 and 73.0 m^2 g_{PtRu}^{-1}, respectively. In principle, these results indicate that Mn(II,III) oxide containing samples have higher number of Pt electroactive sites on the surface of the support to catalyze the electrooxidation of methanol in acid medium. From Fig. 5, it can be noted that the onset potential for CO oxidation on (100-x)C.xMn_3O_4 supported catalysts is slightly lower than that on Mn_3O_4-free sample. This means that the incorporation of Mn(II,III) oxide improves the ability of the bimetallic system for CO oxidation.[28,29]

In several studies where the effect of adding different metal oxides to carbon substrates was tested, activity enhancement was also found. Some proofs were made with CeO_2,[30] $W_{18}O_{49}$,[26] TiO_2,[31] Nb_2O_5,[12] ZrO_2,[32] NiO,[33] among others. The *ECSA* results presented in the current work are comparable to those obtained by Tan et al. for Pt-CeO_2/C and Pt/CeO_2-NiO/C catalysts (66.95 m^2 g^{-1} and 69.06 m^2 g^{-1}, respectively).[30] In comparison, the electroactive surface areas of PtRu/(100-x)C.xMn_3O_4 were calculated to be up to 1.93 times larger than those of the Pt/$W_{18}O_{49}$ catalyst.[26]

The electrocatalytic performance of the as-prepared catalysts was evaluated by cyclic voltammetry from -0.2 to 0.9 V at a sweep rate of 50 mV s^{-1} in 1 M CH_3OH + 0.5 M H_2SO_4 (Fig. 6). The current densities were normalized per milligram of PtRu. The oxidation of adsorbed methanol molecules on the catalyst surface is displayed as an anodic peak centered at ca. 0.7 V in the forward scan, whereas the peak that appears in the reverse scan is associated with the oxidation of intermediate carbonaceous species strongly adsorbed on Pt surface and methanol molecules on reactivated sites.[34]

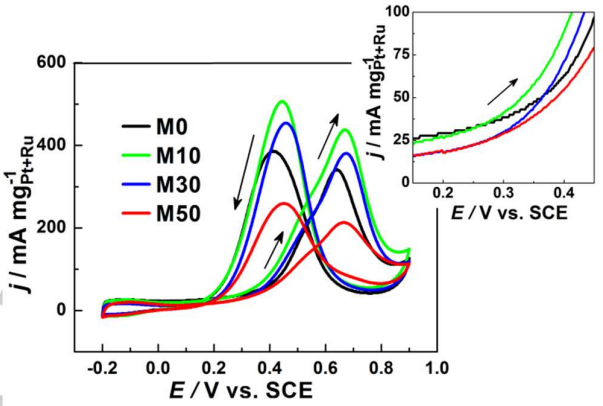

Figure 6. Comparative cyclic voltammograms (thirtieth cycle) of all electrodes in 1 M CH_3OH/0.5 M H_2SO_4 at v = 50 mV s^{-1}. The current response was normalized per milligram of PtRu. The insets show the potential region extended between 0.10 V and 0.50 V.

Both the forward peak current density and the onset potential follow the trend: M10 > M30 > M0 > M50. M10 and M30 electrodes show better catalytic activity than that of M0 sample. In the forward scan, the peak current densities are 437.4 and 380.3 mA mg_{PtRu}^{-1} for M10 and M30 catalysts, respectively; meanwhile it is 341.5 mA mg_{PtRu}^{-1} for M0. The electrochemical experiments indicated that the catalytic activity for methanol oxidation is improved with respect to the PtRu bimetallic system by addition of Mn_3O_4 up to 30 % content. The strong loss of activity observed for M50 and the general trend of decreasing activity M10 > M30 > M50 is attributed to a diminution of the electric conductivity of the hybrid supports by the increasing oxide content. A similar observation was reported elsewhere.[35]

The activity enhancement of samples M10 and M30 can be probably explained in terms of the formation of an additional amount of hydroxyl species onto the surface of Mn_3O_4 nanoparticles as well as onto Ru atoms through the reactions represented by Equations (1) and (2). This specie facilitates the oxidation of reaction intermediates adsorbed on Pt atoms. The equations below summarize the reactions that may take place on the catalysts:

$$Pt\text{-}CH_3OH_{ad} \rightarrow \cdots \rightarrow Pt\text{-}CO_{ad} + 4\,H^+ + 4\,e^- \quad (5)$$

Accepted Manuscript

This article is protected by copyright. All rights reserved.

$Ru\text{-}OH_{ad} + Pt\text{-}CO_{ad} \rightarrow Ru + Pt + CO_2 + H^+ + e^-$ (6)

$Mn_xO_{x+1}\text{-}OH_{ad} + Pt\text{-}CO_{ad} \rightarrow Mn_xO_{x+1} + Pt + CO_2 + H^+ + e^-$ (7)

Despite this hydroxyl specie plays an important role in the bifunctional mechanism, the increase in oxophilicity with the decrease in particle size could lead to a reduction in specific activity, because $–OH_{ad}$ can effectively block the active Pt sites required for the adsorption of methanol molecules.[23]

Another phenomenon that could contribute to the improvement of the catalytic activity involves the previously mentioned hydrogen intercalation/de-intercalation process into Mn_3O_4 lattice. Hence, the methanol dehydrogenation process is catalyzed by Mn^{2+}/Mn^{3+} redox couple via the evolution of protons and electrons.[36,37] Therefore, the utilization of such hybrid support could lead to increase the reaction rate.[26]

Furthermore, the more homogeneous spatial distribution of nanoparticles with the rise in oxide content also contributes to the enhancement of methanol electrooxidation. As commented earlier, the particle distribution is more uniform when the oxide content is higher. The latter is in good agreement with the relationship found between size/distribution and calculated *ECSA* values (Table 2).

Finally, the incorporated oxide can indirectly improve the methanol oxidation. The previous results of CO stripping demonstrated an increase in the electroactive area available for the reaction. The results also showed that the CO_{ad} molecules are oxidized at lower potentials on catalysts M10, M30 and M50 (Fig. 5). The latter is further evidenced when the onset potentials for methanol oxidation are compared in (Fig. 6). Therefore, the platinum sites for the adsorption of methanol molecules on M10, M30 and M50 samples can be released at lower overpotentials than at M0 catalyst.

Furthermore, potentiostatic experiments at 0.4 V and 0.5 V were carried out. The results displayed in Fig. 7 show that the steady state mass current densities of M10 and M30 catalysts are higher than that of M0 electrode.

The electrocatalytic performance of the as-prepared catalysts is acceptable compared with other results found in the literature. For instance, Liu et al. evaluated the catalytic activity of Pt nanoparticles supported on CNT-rGO (nanotubes-reduced graphene oxide). This material reached an activity of 120 mA mg_{Pt}^{-1} at 0.6 V (vs. Ag/AgCl).[38] Vu et al. obtained activities in the range of 25-100 mA mg_{Pt}^{-1} with Pt-AlOOH-SiO_2/graphene hybrid nanomaterials of different composition.[39] A catalyst that consisted of Pt nanoparticles supported on titanium nitride was investigated by Xiao et al.[40] They reported an activity of 64.92 mA mg_{Pt}^{-1} for Pt/TiNi catalyst at 0.6 V (vs. Ag/AgCl). This catalyst exhibited improved activity and stability compared with a commercial Pt/C catalyst.

To complete the information on the effect of Mn_3O_4 in the bimetallic PtRu system, we have determined the poisoning rate (δ, % s^{-1}) of the as-synthesized catalysts in the electrooxidation of methanol by the following equation (8) proposed by Jiang and Kucernak.[41]

$$\delta = (100/I_0) \times (dI/dt)_{t>500\ s} \quad (8)$$

Where $(dI/dt)_{t>500\ s}$ represents the slope of the linear portion of the current decay (A s^{-1}), and I_0 is the current at the start of polarization back extrapolated from the linear current decay (A). The poisoning rate (δ) at 0.4 V resulted to be 0.015, 0.013, 0.021 and 0.044 % s^{-1} for M0, M10, M30 and M50, respectively. Once again, the sample M10 showed the best catalytic behavior because it presents the lowest poisoning rate. That is, M10 has the best ability to oxidize poisoning species thereby releasing Pt active sites of CO molecules and other intermediates species that are generated during methanol electrooxidation. As there are other poisoning species besides CO, it was found that the tendency of δ values differs from that observed in Fig. 5.

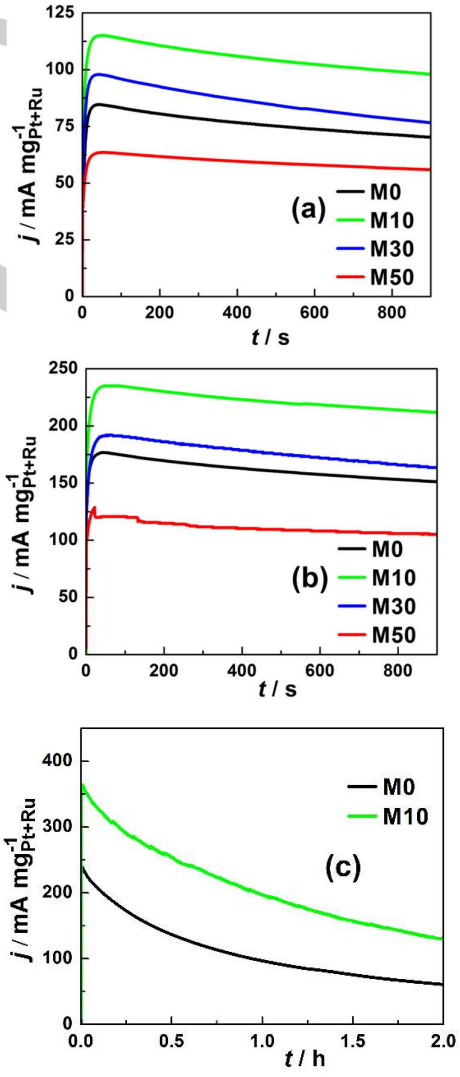

Accepted Manuscript

This article is protected by copyright. All rights reserved.

Figure 7. Chronoamperometric response of the catalysts in 1 M CH_3OH/0.5 M H_2SO_4 at (a) 0.4 V and (b) 0.5 V. Long-term CA curves of M0 and M10 electrodes at 0.5 V (c).

Overall, the utilization of metal oxides offers a variety of oxidation states, the potential for mixed electronic/ionic conduction and the ability to provide a large amount of hydroxyl groups.[15] On the other hand, the generated electron and proton mobility affect overall reactivity. Furthermore, in one way the metal oxides slow down the process of formation of catalytically inactive platinum surface oxides.[42]

Conclusions

In this research, the influence of Mn_3O_4 nanoparticles on the electrocatalytic activity of bimetallic PtRu nanoparticles for methanol oxidation was investigated. The bimetallic PtRu nanoparticles supported over the hybrid carbon-manganese(II,III) supports were successfully synthesized via the microwave-assisted polyol process with ethylene glycol. It was observed that the incorporation of manganese(II,III) oxide nanoparticles onto the carbon support leads to a better particle dispersion, small particle size and absence of agglomerates. The as-prepared catalysts presented similar atomic Pt:Ru ratio, indicating that the composition of the bimetallic system is unaffected by the oxide content in the hybrid support. However, the increase in Mn_3O_4 content leaded to a higher loading of the noble metals over the hybrid support due to the formation of more nucleation sites during the microwave heating.

Cyclic voltammetry and chronoamperometric experiments revealed that among the different studied electrocatalysts the best performance and the lowest poisoning rate were obtained with sample M10 (PtRu/90C.10Mn_3O_4), followed by M30 (PtRu/70C.30Mn_3O_4). This is due to the large electroactive surface area of the nanoparticles deposited over the hybrid supports. On the other hand, the ability of Mn_3O_4 to provide a large extra amount of hydroxyl groups and facilitate the methanol dehydrogenation steps improves the reaction rate of methanol oxidation on the bimetallic PtRu nanoparticles.

In contrast, the electrochemical tests indicated that the activity decreases markedly as the Mn_3O_4 content increases up to 50 wt. % in the hybrid support. This result can be correlated with a strong diminution in the electronic conductivity of the substrate.

Experimental Section

Oxidized carbon black Vulcan XC-72R from Cabot was utilized as support. The pretreatment of the carbonaceous material was carried out with 3.0 M HNO_3 solution at 60 °C for 3 h. The slurry was then cooled and its pH value was adjusted to 7.0 with 1.0 M KOH solution. The carbon powder was then filtered, washed with bidistilled water and ethanol, and dried in an oven at 80 °C overnight. Manganese (II) sulfate monohydrate, NaOH and ethylene glycol (EG, >99 %) were provided by Anedra. Hexachloroplatinic (IV) acid hexahydrate ($H_2PtCl_6{\cdot}6H_2O$, 40 wt. % Pt), potassium hydroxide (KOH, ≥ 85.0 %), sodium borohydride ($NaBH_4$, >94%) tetraethyl orthosilicate (TEOS) and the surfactants cetyltrimethylammonium tosylate (CTAT) and Pluronic F68 were purchased from Sigma-Aldrich. Ruthenium (III) chloride hydrate ($RuCl_3{\cdot}xH_2O$, 41 wt. % Ru) was obtained from Merck. Sulfuric acid (96 wt. %) and hydrochloric acid (37 wt. %) were obtained from Carlo Erba. Methanol (CH_3OH, 99.9%) and isopropyl alcohol (>99.5%) were provided by J.T. Baker®. In addition, Nafion® 117 solution (5 wt. % in a mixture of lower aliphatic alcohols and water) was supplied by Sigma-Aldrich. All solutions were prepared with tridistilled water.

Mn_3O_4 nanoparticles were synthesized in alkaline medium as follows: 40 mL of Pluronic F68-CTAT mixed solution was prepared with a 1:3 molar ratio by adding the desired amount of surfactants to water. This mixture was stirred in a conical flask at 35 ºC to form a transparent template solution and then it was left at room temperature. At the same time, 11.6 mL of a 1.185 M $MnSO_4$ solution were prepared by adding the desired amount of the hydrated salt to water. To obtain the material 20 mL of 1.375 M NaOH were added drop by drop 15 min after the addition of the $MnSO_4$ solution to the surfactant solution. The final pH of the mixture was around 9.8. The resulting product, light brown in coloration and with a $MnSO_4$:NaOH:CTAT:Pluronic F68:H_2O mole composition of 1:2:0.0417:0.0014:289, was stirred for 10 min and then left for 48 h in an autoclave at 100 ºC. Then, the solid was filtered and washed with distilled water and left to dry at room temperature. Finally, it was calcined in an air flux by increasing the temperature from room temperature to 400 °C with a heating rate of 2 °C min^{-1}, and holding for 5 h at 400 °C.

A polyol thermal assisted method (microwave irradiation) was used to synthesize PtRu nanoparticles on a hybrid support composed of carbon black and different amounts of manganese(II,III) oxide ((100-x)C.xMn_3O_4, 0 < x < 50 wt. %). For the preparation, 100 mg of pretreated Vulcan X-72R carbon black and suitable amount of Mn_3O_4 were dispersed in ethylene glycol by magnetic stirring during about 24 h. The dispersion pH was adjusted to ~10 by dropwise addition of 0.5 M KOH-EG solution. Then 38.6 mM H_2PtCl_6 and 20 mM $RuCl_3$ aqueous solutions were added in the mixture under continuous stirring. The deposition of the nanoparticles was achieved by heating the slurry in a microwave oven (2450 MHz, 700 W) under the pulse mode condition of 30 s on/30 s off for four pulses. After that, the mixture was filtered, thoroughly washed and dried overnight at 60 °C. The as-synthesized electrocatalysts were called in the following way: PtRu/100C (M0), PtRu/90C.10Mn_3O_4 (M10), PtRu/70C.30Mn_3O_4 (M30) PtRu/50C.50Mn_3O_4 (M50). To make electrodes, the different supported catalysts were suspended in an ink prepared by ultrasonically blending 20 mg of powder catalysts samples, 7.96 mL of tridistilled water, 2 mL isopropyl alcohol and 20 µL Nafion ionomer solution for 30 min.

X-ray diffraction (XRD, Rigaku Dmax III) with monochromated Cu–Kα radiation source (λ = 0.15418 nm) operated at 40 keV and 30 mA at a scan rate of 0.05 ° s^{-1} with 2θ angles in the range of 20-80 ° was employed to characterize the crystalline structure of the as-prepared PtRu/(100-x)C.xMn_3O_4 catalysts. The peak profiles in XRD patterns of the supported catalysts were fitted with the pseudo-Voigt function, using non-linear least-squares refinement procedures based on a finite difference Marquardt algorithm. The lattice parameters were calculated using Bragg's law and the crystallite sizes estimated using Scherrer's equation. The morphology, distribution and size of the nanoparticles were studied by transmission electron microscopy (TEM, JEOL 100CX II). The particle size (d_p) distribution was determined by measuring the diameter of about 150 particles (only "well defined", not aggregated nanoparticles were taken into account) using the ImageJ image processing and analysis software.[43] The bulk composition was determined by X-ray energy dispersive analysis

Accepted Manuscript

This article is protected by copyright. All rights reserved.

(EDX, LEO 1450VP EDAX). Moreover, the quantitative chemical analysis of the as-prepared catalysts was done using inductively coupled plasma atomic emission spectroscopy (ICP-AES, Shimadzu 1000 model III). For this purpose, 10.0 mg of each sample were digested in aqua regia (3:1 mixture of hydrochloric acid and nitric acid, respectively) for at least 10 h and filtered off to separate the carbonaceous material from the solution containing the metal ions.

The electrochemical experiments were run in conventional three-compartment glass cells with a PAR 273 potentiostat/galvanostat controlled by software ECHEM-M270 at room temperature. The working electrodes were prepared by dispersing 20 µL of the different catalyst inks over glassy carbon electrodes (3 mm diameter) and dried under infrared lamp for 15 min to form a thin film. The reference electrode was a saturated calomel electrode (*SCE*, +0.241 vs. RHE) located in a Luggin capillary and a platinum wire was used as the counter electrode. All solutions were deaerated by bubbling N_2 for 30 min and then the inert atmosphere was maintained over the solution during the tests.

Cyclic voltammetry (CV) and chronoamperometry (CA) techniques were used to evaluate the electrochemical response of the as-prepared catalysts. The CV experiments were carried out first in 0.5 M H_2SO_4 electrolyte solution and then in 1 M CH_3OH + 0.5 M H_2SO_4 solution at a sweep rate of 50 mV s^{-1} for 30 cycles. The potentiostatic experiments (at 0.4 V and 0.5 V) were performed in 1 M CH_3OH + 0.5 M H_2SO_4 solution applying pulses from an initial potential of 0 V for 15 an 120 min. The catalytic activity of the electrodes was normalized in terms of current per unit of active surface area and per mg of PtRu.

CO stripping measurements were done in 0.1 M H_2SO_4 solution. Pure CO was first bubbled into the electrolyte for CO adsorption onto the electrode at -0.091 V and then the excess CO was purged by N_2 bubbling. Next three voltammetry cycles from -0.25 V to 0.8 V at 10 mV s^{-1} were recorded. The initial anodic sweep corresponds to the electrooxidation of CO molecules irreversibly adsorbed onto the electrode surface and it is used to calculate the specific electrochemical active surface area per unit mass of PtRu (*ECSA*). A detailed description of the protocol used in ECSA determination is given elsewhere.[44]

Acknowledgements

This work was supported by ANPCYT grants PICT2013 N°2370 and PICT2014 N° 3393 and Universidad Nacional del Sur grant PGI 24/M142. V.C. thanks CONICET for a doctoral fellowship.

Keywords: Mn_3O_4-Carbon hybrid supports • PtRu nanoparticles • Methanol electrooxidation

[1] M. Li, R.R. Adzic, *Lecture Notes in Energy* **2003**, *9*, 1-25.
[2] S.K. Meher, G.R. Rao, *J. Phys. Chem. C* **2013**, *117*, 4888-4900.
[3] M. Wang, X. Wang, M. Chen, Z. Yang, C. Dong, *Chin. J. Catal.* **2016,** *37*, 1037-1048.
[4] A.M. Sheikh, K.E.A. Abd-Alftah, C.F. Malfatti, *J. Multidiscip. Eng. Sci. Technol.* **2014**,*1*, 1-10.
[5] B. Gurau, R. Viswanathan, R. Liu, T.J. Lafrenz, K.L. Ley, E.S. Smotkin, *J. Phys. Chem. B* **1998**,*102*, 9997-10003.
[6] J. Zhang, H. Liu (Eds.), *Electrocatalysis of direct methanol fuel cells: from fundamentals to applications,* John Wiley & Sons, Weinheim, **2009**.
[7] S. Komarneni, D. Li, B. Newalkar, H. Katsuki, A.S. Bhalla, *Langmuir* **2002**, *18*, 5959-5962.
[8] N.N. Mallikarjuna, R.S. Varma, *Cryst. Growth Des.* **2007**, *7*, 686-690.
[9] E.A. Anumol, P. Kundu, P.A. Deshpande, G. Madras, N. Ravishankar, *ACS Nano* **2011**, *5*, 8049-8061.
[10] A. Nouralishahi, A.A. Khodadadi, Y. Mortazavi, A. Rashidi, M.A. Choolaei, *Electrochim. Acta* **2014**, *147*, 192-200.
[11] R.S. Amin, K.M. El-Khatib, S. Siracusano, V. Baglio, A. Stassi, A.S. Arico, *Int. J. Hydrogen Energy* **2014**, *39*, 9782-9790.
[12] G.R. Rao, P. Justin, S. Meher, *Catal. Surv. Asia* **2011**, *15*, 221-229.
[13] W.Z. Li, L. Kovarik, D. Mei, M.H. Engelhard, F. Gao, J. Liu, Y. Wang, C.H. Peden, *Chem. Mater.* **2014**, *26*, 5475-5481.
[14] Y.H. Qin, Y.F. Li, R.L. Lv, T.L. Wang, W.G. Wang, C.W. Wang, *J. Power Sources* **2015**, *278*, 639-644.
[15] P.J. Kulesza, I.S. Pieta, I.A. Rutkowska, A. Wadas, D. Marks, K. Klak, L. Stobinski, J.A. Cox, *Electrochim. Acta* **2013**, *110*, 474-483.
[16] J.P. Brenet, *J. Power Sources* **1979**, *4*, 183-190.
[17] F.H.B. Lima, M.L. Calegaro, E.A. Ticianelli, *J. Electroanal. Chem.* **2006**, *590*, 152-160.
[18] F.H.B. Lima, M.L. Calegaro, E.A. Ticianelli, *Electrochim. Acta* **2007**, *52*, 3732-3738.
[19] A.M. Castro Luna, G.A. Camara, V.A. Paganin, E.A. Ticianelli, E.R. Gonzalez, *Electrochem. Commun.* **2000**, *2*, 222-225.
[20] J.M. Sieben, M.M.E. Duarte, C.E. Mayer, *ChemCatChem* **2010**, *2*, 182-189.
[21] A. Velázquez-Palenzuela, E. Brillas, C. Arias, F. Centellas, J.A. Garrido, R.M. Rodríguez, P.L. Cabot, *J. Catal.* **2013**, *298*, 112-21.
[22] S. St. John, R.W. Atkinson III, K.A. Unocic, R.R. Unocic, T.A. Zawodzinski Jr, A.B. Papandrew, *ACS Catal.* **2015**, *5*, 7015-7023.
[23] K.J.J. Mayrhofer, B.B. Blizanac, M. Arenz, V.R. Stamenkovic, P.N. Ross, N.M. Markovic, *J. Phys. Chem. B* **2005**,*109*, 14433-14340.
[24] M. Arenz, K.J. Mayrhofer, V. Stamenkovic, B.B. Blizanac, T. Tomoyuki, P.N. Ross, N.M. Markovic, *J. Am. Chem. Soc.* **2005**, *127*, 6819-6829.
[25] A. Wieckowski, J.K. Nørskov (Eds.), *Fuel Cell Science: Theory, Fundamentals, and Biocatalysis*, John Wiley & Sons, Weinhein, **2010**.
[26] F. Li, H. Gong, Y. Wang, H. Zhang, Y. Wang, S. Liu, S. Wang, C. Sun, *J. Mater. Chem. A* **2014**, *2*, 20154-20163.
[27] S. Jayaraman, T.F. Jaramillo, S.H. Baeck, E.W. McFarland, *J. Phys. Chem. B* **2005**, *109*, 22958-22966.
[28] X. Peng, Y. Zhao, D. Chen, Y. Fan, X. Wang, W. Wang, J. Tian, *Electrochim. Acta* **2014**, *136*, 292-300.
[29] C. Zhou, H. Wang, F. Peng, J. Liang, H. Yu, J. Yang, *Langmuir* **2009**, *25*, 7711-7717.
[30] Q. Tan Q, C. Du, Y. Sun, L. Du, G. Yin, Y. Gao, *J. Power Sources* **2014**, *263*, 310-314.
[31] J.-M. Lee, S.-B. Han, J.-Y. Kim, Y.-W. Lee, A.-R. Ko, B. Roh, I. Hwang, K.-W. Park, *Carbon* **2010**, *48*, 2290-2296.
[32] R.S. Amin, A.E. Fetohi, R.M. Abdel Hameed, K.M. El-Khatib, *Int. J. Hydrogen Energy* **2016**, *41*, 1846-1858.
[33] R.S. Amin, R.M. Abdel Hameed, K.M. El-Khatib, M. Elsayed Yousse, A.A. Izatahry, *Electrochim. Acta* **2012**, *59*, 499-508.
[34] J.M. Sieben, V. Comignani, A.E Alvarez, M.M.E. Duarte, *Int. J. Hydrogen Energy* **2014**, *39*, 8667-8674.
[35] X. Yang, X. Wang, G. Zhang, J. Zheng, T. Wang, X. Liu, C. Shu, L. Jiang, C. Wang, *Int. J. Hydrogen Energy* **2012**, *37*, 11167-11175.
[36] J.S. Rebello, P.V. Samant, J.L. Figueiredo, J.B. Fernandes. *J. Power Sources* **2016**, *153*, 36-40.
[37] J. Cai, Y. Huang, B. Huang, S. Zheng, Y. Guo, *Int. J. Hydrogen Energy* **2014**, *39*, 798-807.
[38] G. Liu, Z. Pan, W. Li, K. Yu, G. Xia, Q. Zhao, S. Shi, G. Hu, C. Xiao, Z. Wei, *Appl. Surf. Sci.* **2017**, *410*,70-78.
[39] T.H.T. Vu, T.T.T. Tran, H.N.T. Le, L.T. Tran, P.H.T. Nguyen, N. Essayem, *J. Power Sources* **2015**, *276*, 340-346.
[40] Y. Xiao, Z. Fu, G. Zhan, Z. Pan, C. Xiao, S. Wu, C. Chen, G. Hu, Z. Wei, *J Power Sources* **2015**, *273*, 33-40.
[41] J. Jiang, A. Kucernak, *J. Electroanal. Chem.* **2003**, *543*, 187-199.
[42] K. Lasch, L. Jörissen, J. Garche, *J. Power Sources* **1999**, **84**, 225-230.

Accepted Manuscript

This article is protected by copyright. All rights reserved.

[43] W.S. Rasband, *ImageJ*, U. S. National Institutes of Health, Bethesda, Maryland, USA, https://imagej.nih.gov/ij/, **1997-2016**.

[44] V. Comignani, J.M. Sieben, M.E. Brigante, M.M.E. Duarte, *J. Power Sources* **2015**, *278*, 119-127.

WILEY-VCH

Accepted Manuscript

This article is protected by copyright. All rights reserved.

WILEY-VCH

ARTICLE

Entry for the Table of Contents (Please choose one layout)

ARTICLE

PtRu nanoparticles supported on hybrid manganese(II,III) oxide-carbon composites were prepared by microwave-assisted polyol process with EG. PtRu/90C.10Mn_3O_4 catalyst exhibited a steady current density of 215 mA mg_{PtRu}^{-1} at 0.5 V, which is 40 % higher than that of PtRu/C. Mn_3O_4 particles provides a large extra amount of hydroxyl groups and facilitates CH_3OH dehydrogenation through the Mn^{2+}/Mn^{3+} redox couple via the evolution of H^+ and electrons.

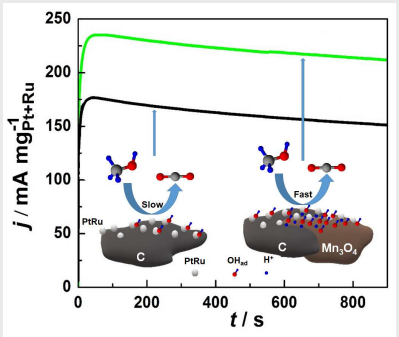

Vanina Comignani, Juan Manuel Sieben, Maximiliano E. Brigante, Marta M.E. Duarte*

Page No. – Page No.

Manganese (II,III) oxide-activated carbon black supported PtRu nanoparticles for methanol electrooxidation in acid medium

Layout 2:

ARTICLE

((Insert TOC Graphic here))

Page No. – Page No.

Accepted Manuscript

This article is protected by copyright. All rights reserved.